Visualization of Subunit-Specific Delivery of Glutamate Receptors to Postsynaptic Membrane during Hippocampal Long-Term Potentiation

AUTHOR(S):

Tanaka, Hiromitsu; Hirano, Tomoo

Please cite this article in press as: Tanaka and Hirano, Visualization of Subunit-Specific Delivery of Glutamate Receptors to Postsynaptic Membrane during Hippocampal Long-Term Potentiation, Cell Reports (2012), doi:10.1016/j.celrep.2012.02.004

Cell Reports
Report

Cell PRESS
Open ACCESS

Visualization of Subunit-Specific Delivery of Glutamate Receptors to Postsynaptic Membrane during Hippocampal Long-Term Potentiation

Hiromitsu Tanaka[1] and Tomoo Hirano[1,*]
[1]Department of Biophysics, Graduate School of Science, Kyoto University, Sakyo-ku, Kyoto 606-8502, Japan
*Correspondence: thirano@neurosci.biophys.kyoto-u.ac.jp
DOI 10.1016/j.celrep.2012.02.004

SUMMARY

An increase in the number of AMPA-type glutamate receptors (AMPARs) is critical for long-term potentiation (LTP), synaptic plasticity regarded as a basal mechanism of learning and memory. However, when and how each type of AMPAR reaches the postsynaptic membrane remain unclear. We have developed experimental methods to form postsynaptic-like membrane (PSLM) on a glass surface to precisely visualize the location and movement of receptors. We observed fluorescence-labeled AMPAR subunits (GluA1–3) around PSLM with total internal reflection fluorescence microscopy. The increases of GluA1, 2, and 3 in PSLM showed different time courses after LTP induction. GluA1 increased first, and was exocytosed to the periphery of PSLM soon after LTP induction. GluA2 and GluA3 initially decreased, and then increased. Exocytosis of GluA2 and GluA3 occurred primarily in non-PSLM, and later than exocytosis of GluA1. Thus, GluA1–3 appear to increase in the postsynaptic membrane through distinct pathways during LTP.

INTRODUCTION

Certain membrane-bound proteins are concentrated in specialized regions of the plasmalemma. They reach their target region via exocytosis from intracellular stores and lateral movement on the plasmalemma, and this trafficking is regulated by external signals and the state of a cell. To understand such processes at the molecular level, direct visualization of the trafficking of membrane-bound molecules with high spatial and temporal resolution can be a powerful tool. Observation of a fluorescent quantum dot bound to a membrane protein through antigen-antibody binding revealed the lateral diffusion of single molecules on the plasmalemma, although this method has not succeeded in visualizing exocytosis (Opazo et al., 2010). Total internal reflection fluorescence microscopy (TIRFM) has been another approach for visualization of such trafficking (Axelrod, 2001). TIRFM selectively excites fluorophores localized very close to a glass surface (~100 nm), thereby reducing the background fluorescence. Thus, TIRFM enables one to observe the translocation of molecules tagged with fluorescent proteins such as EGFP. One problem in using TIRFM has been that in many cases the specialized region of interest in the plasmalemma is not within the evanescent field (the TIRFM visualization zone). Even if it is, the membrane region is usually not formed in parallel to the glass surface and is not static, which makes precise evaluation and quantification of the membrane-bound fluorescent signal difficult. Seeking a way to avoid these problems, we noted that glass coated with proteins of interest through a biotin-streptavidin linker has been successfully used in biochemical studies (Taguchi et al., 2001). Here, we applied a similar glass-coating technique to the plasmalemma of living cells, and formed specialized membrane structure directly on the glass surface, so that fluorescent molecules on the stabilized membrane can be observed with TIRFM. We have applied this method to neuronal synapses in order to address how glutamate receptors are regulated during hippocampal long-term potentiation (LTP).

AMPA (α-amino-3-hydroxy-5-methyl-4-isoxazolepropionic acid)-type glutamate receptors (AMPARs) mediate fast excitatory synaptic transmission in the central nervous system. An increase in the number of AMPARs contributes to the enhancement of synaptic transmission during LTP, a model of synaptic plasticity underlying learning and memory (Malinow and Malenka, 2002; Shepherd and Huganir, 2007). AMPARs are composed of combinations of four subunits: GluA1–4 (Dingledine et al., 1999; Hollmann and Heinemann, 1994). In the hippocampus the predominant AMPARs are GluA1/GluA2 and GluA2/GluA3 heteromers (Derkach et al., 2007; Wenthold et al., 1996). It has been proposed that GluA1 homomer contributes to LTP (Derkach et al., 2007; Plant et al., 2006), although this has been disputed (Adesnik and Nicoll, 2007; Gray et al., 2007). Exocytosis and lateral movement of AMPARs are essential for the increase in the number of AMPARs during LTP induction (Kennedy et al., 2010; Kennedy and Ehlers, 2011; Lin et al., 2009; Makino and Malinow, 2009; Opazo et al., 2010; Opazo and Choquet, 2011; Patterson et al., 2010; Yudowski et al., 2007). However, when and how each type of AMPAR reaches the postsynaptic membrane during LTP remain controversial and elusive. Is GluA1 homomer specifically increased in the early phase of LTP? If so how does GluA1 reach the postsynaptic membrane? When and through what pathway do GluA1/GluA2 and GluA2/GluA3 heteromers increase? To address these questions, we have developed and used new experimental methods.

Cell PRESS
Open ACCESS

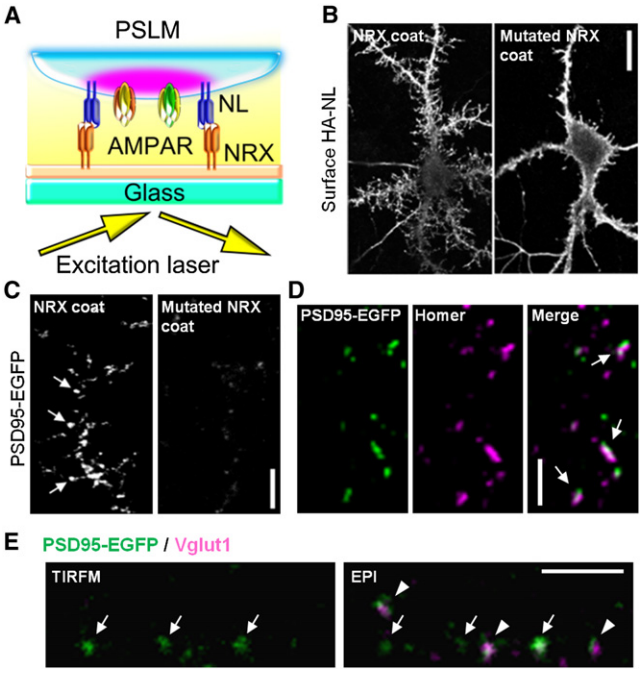

Figure 1. NRX-Coated Glass-Induced PSLM Formation

(A) Schematic drawing of NRX-coated glass and PSLM. NRX is immobilized on the glass surface through biotin-streptavidin and antigen-antibody linkers (beige zone). NRX binds to NL expressed on the neuronal membrane. Postsynaptic scaffold proteins (magenta) and receptors (AMPAR) accumulate near NL in the TIRFM visualization zone (yellow). Yellow arrows indicate excitation laser beam. See also Figure S1.

(B) Representative images of HA-tagged NL-expressing hippocampal neurons cultured on the NRX-coated glass (left) or on the mutated NRX-coated glass (right).

(C) PSD95-EGFP (arrows) was clearly observed with TIRFM on the NRX-coated glass, but not on the mutated NRX-coated glass.

(D) Endogenously expressed Homer (magenta) was colocalized (arrows) with PSD95-EGFP (green) in the TIRFM visualization zone.

(E) The localization of immunostained PSD95-EGFP (green) and Vglut1 (magenta) in the same field was observed with TIRFM (left) or with epi-fluorescence (right). Only PSD95-EGFP (green) was observed (arrows) with TIRFM, whereas other PSD95-EGFP signals were colocalized with Vglut1 (arrowheads) when observed with epi-fluorescence.

Scale bars, 20 μm (B) and 5 μm (C–E).

First, we attempted to form stable postsynaptic membrane directly on a glass surface utilizing synaptic adhesion molecule neurexin (NRX). NRX is a type of presynaptic adhesion molecule that triggers postsynaptic differentiation through binding to postsynaptic neuroligin (NL) (Craig and Kang, 2007; Südhof, 2008). The NRX/NL interaction plays a major role in synaptogenesis. The fact that NRX expressed in non-neuronal cells or attached to beads increases formation of postsynaptic structures (Graf et al., 2004) prompted us to try to use NRX-coated glass for the induction of postsynaptic membrane formation. In this study the postsynaptic-like membrane (PSLM) was formed on the NRX-coated glass, and translocation of AMPAR subunits GluA1–3 in and around PSLM during LTP was studied using TIRFM.

RESULTS

Formation of PSLM on Glass and LTP Induction

We coated cover glass with NRX tagged with immunoglobulin Fc region (Figure 1A; see Figures S1A and S1B available online). Tight coupling of NL on the cell membrane and NRX on the glass was first confirmed using HEK cells that expressed NL tagged with HA (Figures S1C–S1F). When rat hippocampal neurons expressing NL were cultured on the NRX-coated glass, they extended heavily branched dendrites (Figure 1B). PSD95, a marker molecule of glutamatergic postsynaptic density (Sheng and Hoogenraad, 2007), was clearly observed in dendrites with TIRFM (Figure 1C). In contrast when neurons were cultured on the glass coated with mutated NRX lacking the LNS (laminin, NRX, sex hormone-binding globulin) domain, PSD95 was rarely observed. The LNS domain is responsible for binding to NL (Graf et al., 2004). PSLM on the NRX-coated glass also expressed Homer, another marker molecule of glutamatergic postsynaptic density (Sheng and Hoogenraad, 2007) (Figure 1D), suggesting that PSLM was formed directly on the glass. Double visualization of PSD95 and glutamatergic presynaptic marker Vglut1 (vesicular glutamate transporter 1) showed that PSLM on the glass observed with TIRFM was not accompanied by Vglut1 signal but that Vglut1 signal-positive presynaptic varicosities adjacent to PSD95 signals were observed near PSLM with epi-fluorescence (Figure 1E). These results indicate that the NRX-coated glass recruited postsynaptic scaffold proteins and induced formation of PSLM through binding to NL.

Next, we expressed an AMPAR subunit (GluA1, GluA2, or GluA3) fused to Super Ecliptic pHluorin (SEP), a pH-sensitive variant of EGFP, in hippocampal neurons cultured on the NRX-coated glass in order to observe changes of the subunits during LTP. SEP fluorescence is quenched by low pH inside cytoplasmic vesicles such as endosomes, and increases on the plasma membrane (Miesenböck et al., 1998). Neurons were also transfected with NL to facilitate PSLM formation, and with PSD95 labeled with tagRFP (PSD95-RFP) to identify PSLM. Then, electrical field stimulation (1 ms, 50 Hz, 300 stimuli) was applied to induce LTP, presuming that it would induce massive glutamate release from glutamatergic presynaptic terminals near PSLM and that the released glutamate would reach PSLM by diffusion. The stimulation caused an increase in the intracellular Ca^{2+} concentration both in cell bodies and in dendrites, including PSLM, in cultured neurons (Figures S2A–S2D). We also confirmed by whole-cell patch-clamp recording that the field stimulation induced sustained increase of the amplitudes of miniature excitatory postsynaptic currents, suggesting that LTP was induced by the field stimulation at glutamatergic synapses (Figures S2E–S2G).

Changes of GluA1–3 Numbers during LTP

The GluA-SEP signal in dendrites of neurons cultured on the NRX-coated glass was monitored before and every 10 min after the field electrical stimulation, and the signal intensities both inside and outside PSLM were quantified. Here, we defined PSLM as the PSD95-labeled area, including its vicinity (with 320 nm corresponding to two pixels). LTP-inducing stimulation increased the fluorescent signals of GluA1-, GluA2-, and

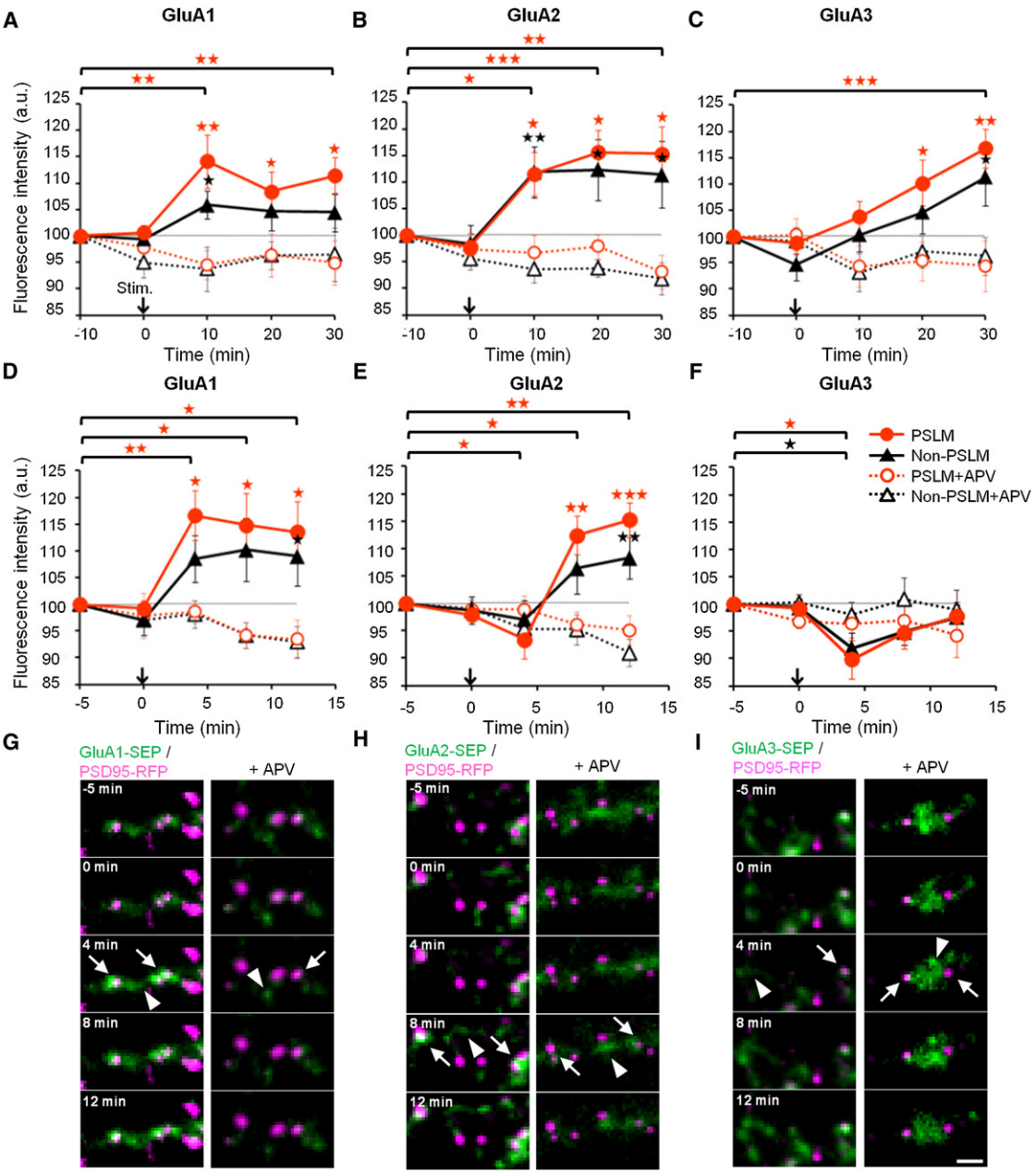

Figure 2. Changes of AMPAR Subunit Number by LTP-Inducing Stimulation

(A–C) Averaged time courses of GluA1–3 fluorescence intensity in PSLM (red) and in non-PSLM (black) measured every 10 min before and after the field stimulation (arrows). Data in the presence of APV (+APV) are also shown (dotted lines). See also Figures S2, S3A, and S3B.

(D–F) Averaged time courses of GluA1–3 fluorescence intensity measured every 4 min. Error bars indicate SEM. Significant differences between −APV and +APV (Dunnett's test), or before and after the stimulation (Steel's test) are marked (n = 8–13 cells; *p < 0.05, **p < 0.01, and ***p < 0.001).

(G–I) GluA-SEP signals (green) and PSD95-RFP signal (magenta) are shown. PSD95-RFP was recorded before the stimulation, and images of detection of the two signals were overlaid. GluA-SEP signals in PSLM and non-PSLM are indicated by arrows and arrowheads, respectively. Scale bar, 2 μm.

GluA3-SEP in PSLM. These increases were suppressed by a blocker of NMDA (N-methyl-D-aspartic acid)-type glutamate receptors, APV (2-amino-5-phosphonovaleric acid) (Figures 2A–2C), which is known to suppress LTP induction (Malinow and Malenka, 2002), and thus the increase in GluA-SEP signal appeared to be related to LTP. The gradual decrease of GluA-SEP signal intensity in the presence of APV was primarily caused by photobleaching (Figures S2H and S2I). In PSLM, GluA1 signal increased and reached a peak at 10 min after the field stimulation, whereas GluA2 signal reached a maximum at 20 min and GluA3 signal at 30 min (Figures 2A–2C). The PSD95-RFP signal, used as a marker for PSLM, rarely moved during the recording,

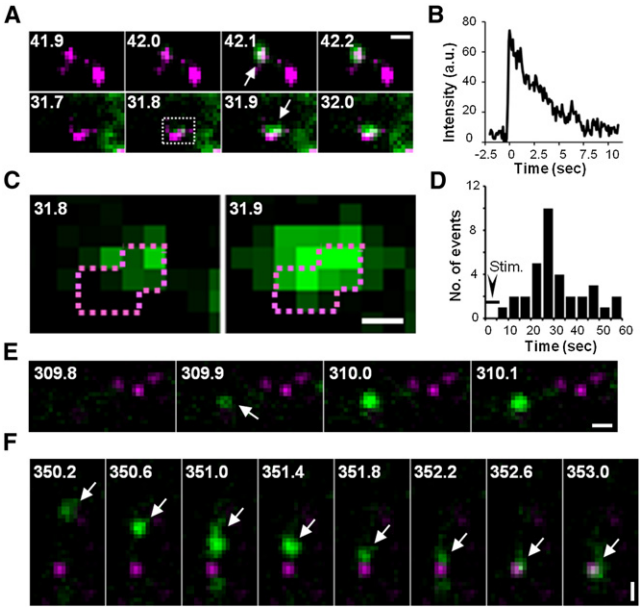

Figure 3. Exocytosis and Lateral Movement of GluA1 and GluA2 during LTP

(A) Two examples of GluA1-SEP (green) exocytosis (arrows) shown together with PSD95-RFP (magenta). The numbers indicate time (seconds) after the field stimulation. The dotted rectangle is enlarged in (C). See also Figures S4A–S4D.

(B) Representative time courses of GluA1-SEP signal intensity before and after the exocytosis.

(C) The left image shows GluA1-SEP appearance in the periphery of PSD95-RFP-positive area (dotted area).

(D) The number of GluA1 exocytosis events within 1 min after the stimulation.

(E) An example of GluA2-SEP (green) exocytosis (arrow) in non-PSLM shown together with PSD95-RFP signal (magenta). See also Figures S4E and 4G.

(F) An example of lateral movement (arrows) of a cluster of GluA2-SEP to PSLM. See also Figures S4F and S4H.

Scale bars, 500 nm (A, E, and F) and 200 nm (C).

suggesting that PSLM itself was stable (Figure S2J). The intensities of GluA1–3 signals in non-PSLM also increased after the stimulation. They were significantly stronger than those with APV, although weaker than those in PSLM. We also examined the effect of chemical induction of LTP (Kennedy et al., 2010; Tao-Cheng et al., 2011; Yudowski et al., 2007), so that all PSLMs would be effectively stimulated. Application of the conditioning solution without Mg^{2+} and containing glycine increased the GluA1-SEP signal in both PSLM and non-PSLM (Figures S3A and S3B).

Next, we analyzed the GluA1–3 signal changes during LTP with a shorter interval (4 min) (Figures 2D–2I). The GluA1 signal in PSLM reached a peak at 4 min after the field stimulation (Figures 2D and 2G). In contrast and intriguingly the GluA2 or GluA3 signal in PSLM initially decreased at 4 min, and then increased or returned to the baseline level at 12 min (Figures 2E, 2F, 2H, and 2I). These results indicate that time courses of the increases of GluA1, GluA2, and GluA3 in PSLM after the LTP-inducing stimulation were different, suggesting that GluA1–3 took different pathways to PSLM.

GluA1–3 Moved to PSLM through Distinct Routes during LTP

To address how GluA1, GluA2, or GluA3 reaches PSLM during LTP, we next performed continuous imaging of the SEP signal. First, GluA1-SEP signal was monitored from the end of field stimulation every 100 ms for 1 min. We observed a rapid increase of GluA1-SEP signal in PSLM, followed by a gradual decrease of the signal (Figures 3A and 3B; Movie S1). This fluorescence emergence occurred in regions where preexisting GluA1-SEP had become undetectable as a result of photobleaching. Careful examination of the images revealed that a large fluorescence increase was preceded by a small increase within the same area (Figure 3C), suggesting that the signal emergence was caused by exocytosis. The presumptive point of exocytosis was not in the center of a PSLM region but rather in its periphery. The distance between the center of a PSD-positive area and that of the exocytosis area was 352 ± 41 nm (n = 34 events). The occurrence of exocytosis in PSLM peaked about 30 s after the stimulation (Figure 3D). We also estimated that the number of exocytosed GluA1 subunits per PSLM region was 2–51 (15 ± 2), judging from the fluorescence intensity of a single SEP molecule (Figures S4A–S4D). The aforementioned results suggest that the LTP-inducing stimulation caused GluA1 exocytosis in the periphery of PSD95-positive areas.

We also observed exocytosis in non-PSLM (Figure S4E). Actually, we recorded a larger number of GluA1 exocytosis events in non-PSLM than in PSLM in the baseline condition (Figure 4A). However, we note that the total measured non-PSLM area (445 ± 71 μm^2) was larger than the total PSLM area (40 ± 7 μm^2) in each experiment. The estimated number of GluA1 subunits exocytosed in non-PSLM was 1–63 (10 ± 2). This value and the exocytosis frequency in non-PSLM are likely to be underestimated because the distance between the cell membrane and the glass seems not to have been constant, and in most non-PSLMs it should have been greater than in PSLM. The lateral movement of GluA1 clusters from non-PSLM to PSLM was also recorded (Figure S4F).

Next, we analyzed the change of frequency of exocytosis after the field stimulation for longer time. For this we performed 0.2 Hz, 5 min continuous monitoring of GluA1-SEP starting at different times after the stimulation (Figure 4A). The frequency of exocytosis in PSLM clearly increased during 0–1 min after the stimulation. In non-PSLM the frequency of GluA1 exocytosis peaked between 0 and 1 min and between 4 and 5 min after the stimulation. We also examined GluA1-SEP exocytosis during and after the chemical induction of LTP (Figure S3C). The exocytosis frequency increased during the period of 0–5 min in PSLM and 0–6 min in non-PSLM. Thus, it was confirmed that exocytosis of GluA1 occurred more frequently after LTP induction, although a sharp peak of the frequency increase was not detected with chemical induction.

We next monitored GluA2-SEP movement by 1 min, 10 Hz continuous imaging starting at various times after the stimulation. We failed to observe an exocytosis-like rapid increase of GluA2-SEP signal in PSLM for the first 5 min, but such an increase occurred in non-PSLM (Figure 3E). The estimated number of GluA2 subunits exocytosed in non-PSLM was 2–22 (9 ± 1, n = 26 events). We also observed translocation of a cluster

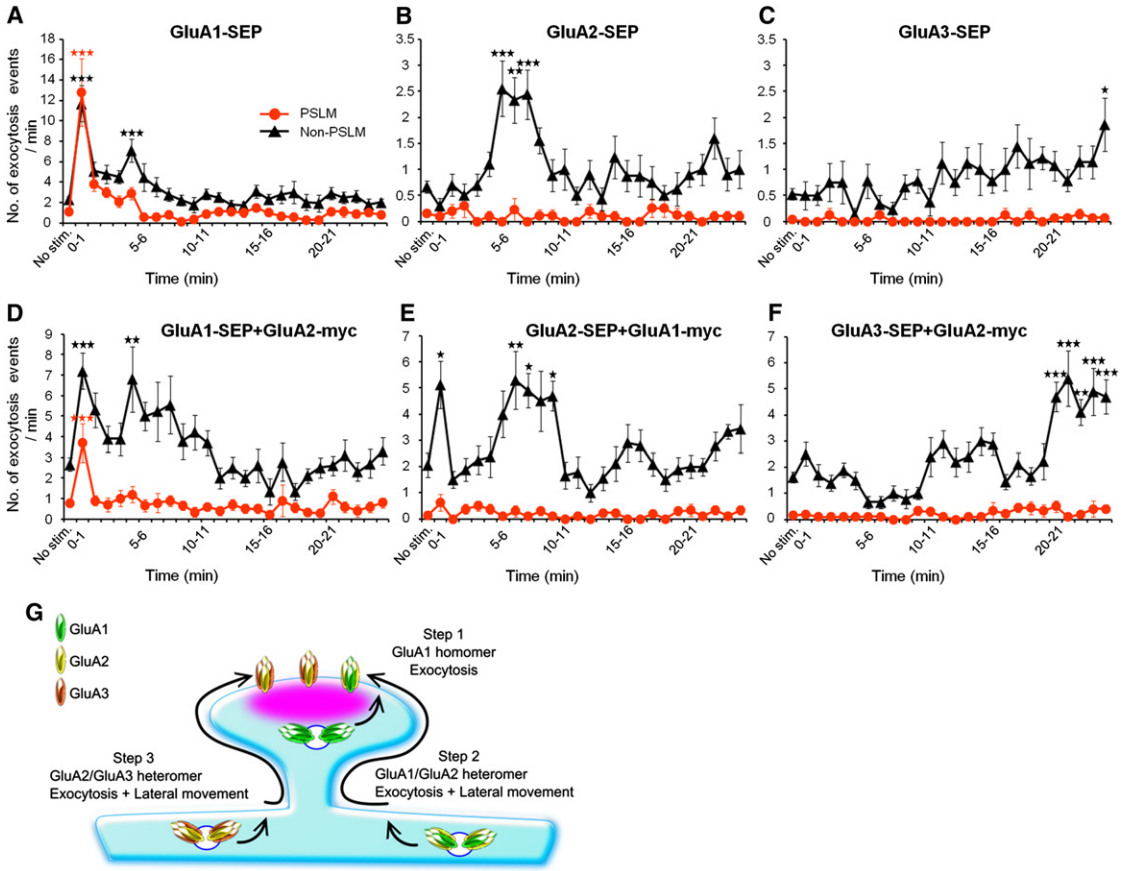

Figure 4. Frequency of GluA1–3 Exocytosis during LTP

(A–F) The time courses of exocytosis frequency of GluA1-SEP (A and D), GluA2-SEP (B and E), and GluA3-SEP (C and F) in PSLM (red) and in non-PSLM (black) are presented (n = 8–13 cells; *p < 0.05, **p < 0.01, and ***p < 0.001, compared to no stimulation [No stim.], Dunnett's test). In (A)–(C), GluA1-, GluA2-, or GluA3-SEP was expressed alone. In (D), GluA1-SEP was coexpressed with GluA2 labeled with myc tag (GluA2-myc), in (E), GluA2-SEP was coexpressed with GluA1-myc, and in (F), GluA3-SEP was coexpressed with GluA2-myc. See also Figure S3C.

(G) A hypothetical scheme of postsynaptic delivery of AMPARs during LTP.

of GluA2-SEP signal from non-PSLM to PSLM (Figure 3F; Movie S2). These results suggest that the increase of GluA2 in PSLM that occurred several minutes after the LTP-inducing stimulation was partly attributable to the lateral movement of GluA2 exocytosed in non-PSLM. Recording of the whole translocation process was not possible in many cases because of the fast photobleaching of SEP and the variable distance between the cell membrane and the glass in non-PSLM.

We next performed 5 min, 0.2 Hz monitoring of GluA2-SEP (Figure 4B). We observed a larger number of exocytosis events in non-PSLM, and a few in PSLM with this recording method. Thus, GluA2 exocytosis primarily took place in non-PSLM. The frequency of GluA2 exocytosis in non-PSLM was less than that of GluA1, and it was significantly increased for 5–8 min after the stimulation. This timing was nearly coincident with the second peak of GluA1 exocytosis in non-PSLM (Figure 4A).

Next, we recorded GluA3-SEP exocytosis. The 10 Hz, 1 min continuous recording detected GluA3 exocytosis only in non-PSLM (Figure S4G), and the estimated number of GluA3 exocytosed at an event was 2–7 (5 ± 0.3, n = 15 events). Translocation of GluA3-SEP from non-PSLM to PSLM was also observed (Figure S4H). The 0.2 Hz, 5 min monitoring of GluA3-SEP confirmed that the exocytosis occurred mainly in non-PSLM, and exocytosis in PSLM was very rare. The frequency of GluA3-SEP exocytosis in non-PSLM was less than that of GluA1 throughout the recordings. It did not increase for the first 10 min. A significant increase was detected at 24–25 min after the stimulation (Figure 4C).

The aforementioned results about exocytosis might have been biased by overexpression of a single type of GluA subunit. To evaluate the effect of unbalanced expression of GluA subunits, we next performed coexpression of GluA1 and GluA2, or GluA2 and GluA3 (Figures 4D–4F). Even when GluA1 and GluA2 were coexpressed, GluA1 exocytosis in the periphery of PSLM soon after the stimulation was observed (Figure 4D), and GluA2 exocytosis in the periphery of PSLM was rare (Figure 4E), supporting the notion that only homomeric GluA1 receptor was exocytosed in the periphery of PSLM. The increased frequency of both GluA1 and GluA2 exocytosis in non-PSLM about 5 min after the stimulation (Figures 4D and 4E) suggests that at this

time GluA1/GluA2 heteromer was exocytosed in the extrasynaptic membrane. Interestingly, in this coexpression experiment the frequency of GluA2 exocytosis in non-PSLM significantly increased soon after the stimulation, suggesting that GluA1/GluA2 heteromer was exocytosed at this time when both GluA1 and GluA2 were equally expressed. The GluA2 and GluA3 coexpression experiment demonstrated that GluA3 exocytosis clearly increased from about 20 min after the stimulation (Figure 4F), suggesting that exocytosis of GluA2/GluA3 heteromer took place >20 min after the stimulation.

DISCUSSION

PSLM Formation in TIRFM Visualization Zone

We have introduced methods applying TIRFM to observe fluorescently tagged AMPAR around PSLM. This method allowed us to record fluorescence signal changes with a high signal to noise ratio, spatial and temporal resolution, and also made it possible to estimate the number of exocytosed AMPAR subunits. In this method, PSLM was formed stably in parallel to the glass surface. Thus, fluorescence signal changes should have been influenced neither by movement of the cell membrane nor by changes of the angle between the membrane and the glass surface, thus making it possible to precisely determine AMPAR localization and exocytosis points, and also signal intensities. One drawback of our method is that PSLM would be different from native postsynaptic structures in some respects. However, the presence of PSD95 and Homer, and the accumulation of GluA1–3 signals, suggest that PSLM retains essential properties of the glutamatergic postsynaptic membrane. Another limitation of this method is the flickering and relatively fast photobleaching of SEP fluorescence (Yudowski et al., 2007), which prevented stable long-term recording and made it difficult to trace a single molecule's movement.

We recorded exocytosis by continuous 10 Hz, 1 min recordings and also by 0.2 Hz, 5 min recordings. The former recording provided better time resolution and clarified the detailed exocytosis process, although the fluorescent signal decayed faster. On the other hand, the latter method allowed longer recordings at the cost of time resolution. It allowed us to detect more exocytosis events (Araki et al., 2010). However, in this recording condition the detailed processes of exocytosis and lateral movement were not reliably recorded.

Previous studies using TIRFM did not observe GluA1 exocytosis in the periphery of the postsynaptic membrane, but only in extrasynaptic membrane (Lin et al., 2009; Yudowski et al., 2007), whereas Kennedy et al. (2010) demonstrated GluA1 exocytosis in the periphery of postsynaptic membrane with confocal microscopy. The formation of PSLM on the glass in the present study might have facilitated detection of exocytosis in the periphery of postsynaptic membrane with TIRFM. We also note that GluA1 exocytosis in the periphery of PSLM occurred only in a limited time window. Chemical induction of LTP also increased the amount of GluA1 and the frequency of GluA1 exocytosis, but the timing of the increase in GluA1 exocytosis frequency in PSLM soon after the stimulation was unclear (compare Figure 4A and Figure S4B). Thus, the electrical stimulation provided better control of the timing of LTP induction than bath application of chemicals. We think that the experimental methods described here will be useful for future studies focusing on the location, movement, and interactions of molecules in the postsynaptic membrane. The methods could also contribute to analyzing the movement and interactions of plasma membrane-bound molecules in various other cell types.

Delivery of GluA1 to Postsynaptic Membrane during LTP

We showed that GluA1 increased within a few minutes after the LTP-inducing stimulation, and that GluA1 exocytosis in the periphery of PSLM frequently occurred around 30 s after the stimulation, and thus seems to contribute to the initial phase of LTP. At this time, GluA1 exocytosis but not GluA2 exocytosis was observed in the periphery of PSLM when GluA1 and GluA2 were expressed together. This suggests that only GluA1 homomer can be specifically exocytosed in the periphery of PSLM soon after the LTP induction, even if both GluA1 and GluA2 are equally expressed. We also observed GluA1 exocytosis in non-PSLM, and its frequency increased after the LTP induction. The GluA1 exocytosis in non-PSLM paralleled GluA2 exocytosis, suggesting that it reflects the exocytosis of GluA1/GluA2 heteromer. Thus, there seem to be multiple routes for trafficking of GluA1 to the postsynaptic membrane.

Plant et al. (2006) reported an increase of GluA2-lacking AMPARs in the early phase of LTP, followed by replacement by GluA2-containing AMPARs. Previous studies showed GluA1 incorporation into the postsynaptic structures during LTP (Hayashi et al., 2000; Kopec et al., 2006). Thus, it has been considered that the number of GluA1 homomers with a high mean single-channel conductance (Kristensen et al., 2011) increases during LTP, although this idea has been disputed by authors (Adesnik and Nicoll, 2007; Gray et al., 2007), who failed to detect GluA2-lacking AMPAR in the hippocampal LTP, implying that the increased frequency of GluA1 homomer exocytosis in the periphery of PSLM might be an artifact caused by overexpression of GluA1. Our finding that the frequency of GluA1 exocytosis in the periphery of PSLM was higher when only GluA1 was overexpressed than when both GluA1 and GluA2 were overexpressed might be a clue to understanding how the difference emerged. We think that hippocampal neurons have the molecular machinery to support selective exocytosis of GluA1 homomer immediately after the LTP induction in the periphery of the postsynaptic membrane. However, the extent of contribution of this exocytosis machinery to LTP may be determined by the relative expression levels of GluA1 and GluA2, which are likely to be influenced by the type, age, and/or condition of neurons.

Delivery of GluA2 and GluA3 to Postsynaptic Membrane during LTP

Translocation of GluA2 during LTP has been studied (Passafaro et al., 2001; Araki et al., 2010; Tao-Cheng et al., 2011). Passafaro et al. (2001), using a thrombin cleavage assay, suggested that GluA2 is inserted more directly into synapses than GluA1, although the time and spatial resolutions were limited, and exocytosis was not directly observed in their study. In a recent study using electron microscopy, Tao-Cheng et al. (2011) found that GluA2 exocytosis occurred only in extrasynaptic membrane,

and that the frequency was increased by application of glycine or a high concentration of K^+. Our finding that GluA2 exocytosis was primarily observed only in non-PSLM is in line with the latter report. The timing of GluA2 exocytosis during LTP has remained relatively unclear. We showed here that the frequency of GluA2 exocytosis increased soon after, and again several minutes after, the stimulation. GluA2 seems to increase in the postsynaptic membrane later than GluA1 during LTP, as previously suggested by Plant et al. (2006). In addition we detected a slight decrease of GluA2 signal at 4 min after the stimulation. It is possible that this decrease of GluA2 provides space for GluA1 homomer, which is incorporated into the postsynaptic membrane in the initial phase of LTP. The lateral movement of a cluster of GluA2 to PSLM was also recorded, and would contribute to the increase of GluA2 in PSLM. These results also suggest that AMPARs on the cell membrane might be translocated to the postsynaptic membrane by a mechanism more complex than a single-molecular lateral diffusion in some cases. However, the quantitative evaluation of translocation in non-PSLM was difficult. The relatively fast photobleaching of fluorescent SEP prevents stable recording of the translocation of weak signals.

Presently, little if any information is available about the translocation of GluA3 during LTP. Here, we showed that the GluA3 signal increased in PSLM. The increase occurred later than the increase of GluA1 and GluA2, and it was accompanied by an increase of the signal in non-PSLM. The initial decrease of GluA3 signal together with that of GluA2 and the rapid increase of GluA1 signal (Figure 2) suggest that GluA2/GluA3 heteromer might be removed from PSLM and replaced by GluA1 homomer in the initial phase of LTP. Most of the GluA3 exocytosis occurred in non-PSLM, like that of GluA2, and the frequency of GluA3 exocytosis increased later than that of GluA2. The fact that the increase in GluA3 exocytosis frequency at times later than 20 min after the stimulation was made clearer by coexpression of GluA2 suggests that GluA3 exocytosis reflects the exocytosis of GluA2/GluA3 heteromer.

Taking into account all of the present observations, we would like to propose the following hypothetical scheme for the postsynaptic delivery of AMPARs during LTP (Figure 4G). Mainly, GluA1 homomer is exocytosed to the vicinity of the postsynaptic membrane within 1 min after the LTP-inducing stimulation, contributing to the initial phase of LTP. During this time, removal of GluA2/GluA3 heteromer in the postsynaptic membrane might also occur, providing slots into which GluA1 homomer would be incorporated. In addition, exocytosis of GluA1/GluA2 heteromer in the extrasynaptic membrane followed by lateral movement to the postsynaptic membrane also seems to occur. About 5 min later, GluA1/GluA2 heteromer is exocytosed to the extrasynaptic membrane and then translocated to the postsynaptic membrane again. More than 20 min later, the frequency of exocytosis of GluA2/GluA3 heteromer to the extrasynaptic membrane increases, contributing to the later increase of GluA3 in the postsynaptic membrane.

EXPERIMENTAL PROCEDURES

NRX labeled with human immunoglobulin Fc fragment was obtained from NRX-transfected HEK293T cells using nProtein A Sepharose (GE Healthcare), and immobilized on the glass surface by the binding reaction of biotin and streptavidin, and by antigen-antibody reaction (Figures S1A and S1B). Hippocampal neuronal culture was prepared from E18–E20 rat embryos, and neurons were transfected with NL labeled with HA, PSD95-RFP, and AMPAR subunit (GluA1, GluA2, or GluA3) labeled with SEP at 10–15 days in vitro. Live imaging of the fluorescence signal was performed by TIRFM at room temperature (22°C–26°C) 1–2 days after transfection. Electrical field stimulation was applied to induce LTP, and GluA-SEP signal changes in both PSLM and non-PSLM were monitored every 4 or 10 min after the stimulation. We also performed 10 Hz, 1 min or 0.2 Hz, 5 min imaging of GluA-SEP signals. The number of exocytosed GluA1–3 subunits was estimated by comparing with the fluorescence intensity of a single SEP molecule. Single-molecule analysis was performed using MetaMorph (Molecular Devices). All experiments were performed according to the guidelines for animal experimentation by the National Institutes of Health (United States) and Kyoto University, and all procedures were approved by the local committee for handling experimental animals at the Graduate School of Science, Kyoto University. More detailed description of experimental procedures is available in the Extended Experimental Procedures.

SUPPLEMENTAL INFORMATION

Supplemental Information includes Extended Experimental Procedures, four figures, and two movies and can be found with this article online at doi:10.1016/j.celrep.2012.02.004.

LICENSING INFORMATION

ACKNOWLEDGMENTS

We thank S. Kawaguchi, Y. Tagawa, Y. Fukazawa, Y. Kubo, and E. Nakajima for comments on the manuscript. This research was supported by grants-in-aid for scientific research from Japan Society for the Promotion of Science, and from the Ministry of Education, Culture, Sports, Science and Technology in Japan, and also by Global COE program A06 of Kyoto University.

Received: September 21, 2011
Revised: December 28, 2011
Accepted: February 9, 2012
Published online: March 22, 2012

REFERENCES

Adesnik, H., and Nicoll, R.A. (2007). Conservation of glutamate receptor 2-containing AMPA receptors during long-term potentiation. J. Neurosci. *27*, 4598–4602.

Araki, Y., Lin, D.T., and Huganir, R.L. (2010). Plasma membrane insertion of the AMPA receptor GluA2 subunit is regulated by NSF binding and Q/R editing of the ion pore. Proc. Natl. Acad. Sci. USA *107*, 11080–11085.

Axelrod, D. (2001). Total internal reflection fluorescence microscopy in cell biology. Traffic *2*, 764–774.

Craig, A.M., and Kang, Y. (2007). Neurexin-neuroligin signaling in synapse development. Curr. Opin. Neurobiol. *17*, 43–52.

Derkach, V.A., Oh, M.C., Guire, E.S., and Soderling, T.R. (2007). Regulatory mechanisms of AMPA receptors in synaptic plasticity. Nat. Rev. Neurosci. *8*, 101–113.

Dingledine, R., Borges, K., Bowie, D., and Traynelis, S.F. (1999). The glutamate receptor ion channels. Pharmacol. Rev. *51*, 7–61.

Graf, E.R., Zhang, X., Jin, S.X., Linhoff, M.W., and Craig, A.M. (2004). Neurexins induce differentiation of GABA and glutamate postsynaptic specializations via neuroligins. Cell *119*, 1013–1026.

Gray, E.E., Fink, A.E., Sariñana, J., Vissel, B., and O'Dell, T.J. (2007). Long-term potentiation in the hippocampal CA1 region does not require insertion and activation of GluR2-lacking AMPA receptors. J. Neurophysiol. *98*, 2488–2492.

Hayashi, Y., Shi, S.H., Esteban, J.A., Piccini, A., Poncer, J.C., and Malinow, R. (2000). Driving AMPA receptors into synapses by LTP and CaMKII: requirement for GluR1 and PDZ domain interaction. Science *287*, 2262–2267.

Hollmann, M., and Heinemann, S. (1994). Cloned glutamate receptors. Annu. Rev. Neurosci. *17*, 31–108.

Kennedy, M.J., and Ehlers, M.D. (2011). Mechanisms and function of dendritic exocytosis. Neuron *69*, 856–875.

Kennedy, M.J., Davison, I.G., Robinson, C.G., and Ehlers, M.D. (2010). Syntaxin-4 defines a domain for activity-dependent exocytosis in dendritic spines. Cell *141*, 524–535.

Kopec, C.D., Li, B., Wei, W., Boehm, J., and Malinow, R. (2006). Glutamate receptor exocytosis and spine enlargement during chemically induced long-term potentiation. J. Neurosci. *26*, 2000–2009.

Kristensen, A.S., Jenkins, M.A., Banke, T.G., Schousboe, A., Makino, Y., Johnson, R.C., Huganir, R., and Traynelis, S.F. (2011). Mechanism of Ca^{2+}/calmodulin-dependent kinase II regulation of AMPA receptor gating. Nat. Neurosci. *14*, 727–735.

Lin, D.T., Makino, Y., Sharma, K., Hayashi, T., Neve, R., Takamiya, K., and Huganir, R.L. (2009). Regulation of AMPA receptor extrasynaptic insertion by 4.1N, phosphorylation and palmitoylation. Nat. Neurosci. *12*, 879–887.

Makino, H., and Malinow, R. (2009). AMPA receptor incorporation into synapses during LTP: the role of lateral movement and exocytosis. Neuron *64*, 381–390.

Malinow, R., and Malenka, R.C. (2002). AMPA receptor trafficking and synaptic plasticity. Annu. Rev. Neurosci. *25*, 103–126.

Miesenböck, G., De Angelis, D.A., and Rothman, J.E. (1998). Visualizing secretion and synaptic transmission with pH-sensitive green fluorescent proteins. Nature *394*, 192–195.

Opazo, P., and Choquet, D. (2011). A three-step model for the synaptic recruitment of AMPA receptors. Mol. Cell. Neurosci. *46*, 1–8.

Opazo, P., Labrecque, S., Tigaret, C.M., Frouin, A., Wiseman, P.W., De Koninck, P., and Choquet, D. (2010). CaMKII triggers the diffusional trapping of surface AMPARs through phosphorylation of stargazin. Neuron *67*, 239–252.

Passafaro, M., Piëch, V., and Sheng, M. (2001). Subunit-specific temporal and spatial patterns of AMPA receptor exocytosis in hippocampal neurons. Nat. Neurosci. *4*, 917–926.

Patterson, M.A., Szatmari, E.M., and Yasuda, R. (2010). AMPA receptors are exocytosed in stimulated spines and adjacent dendrites in a Ras-ERK-dependent manner during long-term potentiation. Proc. Natl. Acad. Sci. USA *107*, 15951–15956.

Plant, K., Pelkey, K.A., Bortolotto, Z.A., Morita, D., Terashima, A., McBain, C.J., Collingridge, G.L., and Isaac, J.T.R. (2006). Transient incorporation of native GluR2-lacking AMPA receptors during hippocampal long-term potentiation. Nat. Neurosci. *9*, 602–604.

Sheng, M., and Hoogenraad, C.C. (2007). The postsynaptic architecture of excitatory synapses: a more quantitative view. Annu. Rev. Biochem. *76*, 823–847.

Shepherd, J.D., and Huganir, R.L. (2007). The cell biology of synaptic plasticity: AMPA receptor trafficking. Annu. Rev. Cell Dev. Biol. *23*, 613–643.

Südhof, T.C. (2008). Neuroligins and neurexins link synaptic function to cognitive disease. Nature *455*, 903–911.

Taguchi, H., Ueno, T., Tadakuma, H., Yoshida, M., and Funatsu, T. (2001). Single-molecule observation of protein-protein interactions in the chaperonin system. Nat. Biotechnol. *19*, 861–865.

Tao-Cheng, J.H., Crocker, V.T., Winters, C.A., Azzam, R., Chludzinski, J., and Reese, T.S. (2011). Trafficking of AMPA receptors at plasma membranes of hippocampal neurons. J. Neurosci. *31*, 4834–4843.

Wenthold, R.J., Petralia, R.S., Blahos J, I.I., and Niedzielski, A.S. (1996). Evidence for multiple AMPA receptor complexes in hippocampal CA1/CA2 neurons. J. Neurosci. *16*, 1982–1989.

Yudowski, G.A., Puthenveedu, M.A., Leonoudakis, D., Panicker, S., Thorn, K.S., Beattie, E.C., and von Zastrow, M. (2007). Real-time imaging of discrete exocytic events mediating surface delivery of AMPA receptors. J. Neurosci. *27*, 11112–11121.